Applied Chemical Engineering (2025) Volume 8 Issue 2 ISSN: 2578-2010 (O)
doi: 10.59429/ace.v8i2.5671

RESEARCH ARTICLE

Extraction and spectroscopic determination of Ni (ll) as a chelation complexes using new azo reagents

Alaa Jawad Abdulzuhraaa[1*], Safa Majeed Hameedb[2]

1. Department of Pharmaceutical Chemistry, Faculty of Pharmacy, University of Kufa, Najaf, Iraq*

2. Department of Chemistry, Faculty of Education for Women, University of Kufa, Iraq

***Corresponding author:** Alaa Jawad Abdulzuhraaa, alaaj.alkhaqani@student.uokufa.edu.iq

ABSTRACT

A highly sensitive approach for separating and determining the micro amount of nickel (II) was conducted. It has been achieved after the formation of chelation complexes with 4-((4-hydroxyquinolin-3-yl) diazenyl) benzenesulfonamide (HQDBS) and 3-((1H-indol-5-yl)diazenyl)quinolin-4-ol (IDQ) as complexing agents (which are examined by using UV-Vis., FT-IR, and ^{1}HNMR spectrum), including joint cloud point extraction with liquid ion exchange methods in the presence of the nonionic surfactant Triton X–100. The study is based on the wavelength values of maximum absorbance, λ_{max} = 480 and 484 nm, respectively. The study optimized the extraction conditions, including the reagent concentration, temperature, heating duration, and surfactant volume. The concentration of reagents for achieving higher extraction efficiency is 1×10^{-3} M in the presence of 100 µg Ni (II)/mL of aqueous solution. The solutions should be heated at 80°C and 90°C HQDBS and IDQ respectively, for 15 minutes. The optimal volume of surfactants is 0.8 mL of Triton X-100 with HQDBS and 0.5 mL with IDQ. The study also includes an analysis of the impact of electrolytes and interferences and the spectrophotometric identification of Ni (II) in various samples.

Keywords: chelation complex; spectrophotometric studies; surfactant; and cloud point extraction

ARTICLE INFO

Received: 16 May 2025
Accepted: 20 May 2025
Available online: 16 June 2025

1. Introduction

Human civilization confronts a substantial difficulty posed by environmental contamination[1]. Environmental pollution and toxic metal poisoning pose substantial risks to human health[2] and the ecosystems[3,4]. The repid development in industrial sector[5,6] including textile, battery production, leather tanning, jewelry as well as paper industries[7] are mainly responsible for discharging heavy metals to waterbodies[8-10]. These heavy metals when present in water system, they are major cause of affecting both human health and the environment[11,12]. For removing heavy metals especially nickel (Ni) from water, several conventional techniques have been developed which include electrolysis[13-15], reverse osmosis or membrane filtration[11], ion exchange[16,17], chemical precipitation, as well as adsorption[18-20]. Nevertheless, all these processes find limitations on a larger scale that might be due to high cost and advanced technique for their operation[21,22]. An efficient method for detecting trace nickel (Ni (II)) and its separating is Cloud point extraction (CPE). This is the most convenient method and find extensive uses due to its less cost, and flexibility towards variety of samples[23-27].

This method involves two different processes: In the first technique, metal ions are present in a compound with an appropriate ligand. Another approach is the straight implementation of the CPE operation devoid of ligands. Azo dyes, characterized by one or more azo groups (-N=N-), comprise the most extensive category of industrially produced organic dyes, owing to their many uses in textile fiber dyeing, photochromism, and advanced chemical synthesis[28-31]. Recent years have witnessed the development of novel and eco-friendly catalytic techniques for synthesizing azo-derived chemicals, which have been utilized as sensors for detecting metal ions. These compounds' significant pharmacological and biological features make them particularly intriguing for research[32-36].

This study aimed to develop a sensitive, selective, and efficient method for Ni (II) determination in environmental and industrial samples, achieved through the synthesis of novel azo reagents, HQDBS and IDQ, designed for effective Ni (II) chelation. To maximize extraction efficiency, key parameters like pH, reagent concentration, temperature, surfactant volume, and heating duration were meticulously optimized. Different techniques as UV-Vis, FTIR, 1H-NMR were used for analysis. Additionally, the study demonstrate that cloud point extraction can be an effective method for analysis of trace metals when used with novel azo reagents, HQDBS and IDQ. By combining several spectroscopic techniques to thoroughly analyze the complexes, we've strengthened the validity of our results. This work contributes to the advancement of metal ion extraction and analysis, providing a practical and scalable solution for environmental and industrial applications.

2. Materials and methods

2.1. Chemicals and materials

The current investigation utilized a Biochrom double beam UV-visible spectrophotometer (S60 Biochrom Libra, Cambridge, United Kingdom), an Electrostatic water bath (G, Gerhardt, Germany), a WTW Laboratory Equipment pH meter (E163694, Germany) and an A&D Company. Limited electronic balance (CE, Dool, HR 200, Japan) were employed. All compounds were employed as obtained from the commercial source without any purification. Solutions were formulated using double-distilled water.

2.2. Synthesis of azo compound

The organic reagents HQDBS and IDQ were synthesized in the laboratory following the method described by Shibata et al. (Scheme 1)[27]. This process involves dissolving 1.722 g (0.01 mole) of sulfanilamide and 1.32g (0.01 mole) of 5-amino indole in a solution containing 25 mL distilled water and 4 mL concentrated HCl. Upon cooling the solution to a temperature range of 0-5°C, 0.7g of sodium nitrite was introduced, dissolving it in 10 mL of distilled water while sustaining the temperature at 0°C. The mixture was let to rest for 15 minutes to complete the diazotization. The diazonium solution was meticulously introduced dropwise to a solution of 1.451 g (0.01 mole) of 4-hydroxyquinoline, dissolved in 10% NaOH and 20 mL of ethanol, while sustaining the temperature at 0°C. Once the addition was complete, the solution was left to stand for two hours. Distilled water was then introduced, and the pH of the solution was adjusted to 6 using HCl. Orange molecules were precipitated and left to stand for 24 hours.

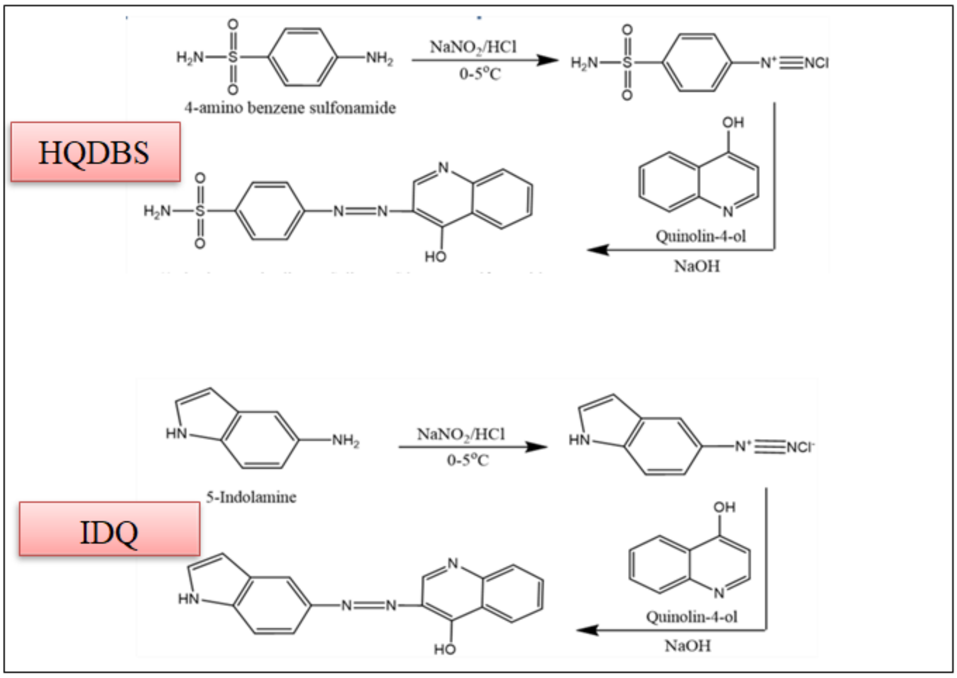

Scheme 1. Schematic illustration of HQDBS and IDQ reagents.

2.3. Solution preparation

A standard 100 µg/mL Ni (II) ion solution was generated by dissolving 0.022 g of $NiCl_2.6H_2O$ (99% from LAB-SCAN) in 100 mL of distilled water only. Solutions of organic reagents HQDBS and IDQ (1×10^{-3} M) were produced by dissolving 0.008 g and 0.0072 g, respectively, in 25 mL of distilled water—any alternative effective solutions developed via repeated dilution with distilled water to the requisite volume.

2.4. Procedure

10 mL aqueous solutions were created utilizing 100 µg/mL Ni(II) and (1×10^{-3} M) derived from an organic reagent. An appropriate 1% Triton X100 amount was included as a nonionic surfactant. The solution was heated in the electrostatic bath of water at an adequate temperature and time. The CPL was removed from the aqueous solution and then dissolved in 5 mL of ethanol. Thereafter, the absorbance was measured utilizing ethanol as a blank at λ_{max}. The aqueous solution underwent treatment using the dimethyl glyoxime spectrophotometric technique to quantify the residual Ni (II) in the aqueous phase post-extraction and to compute the distribution ratio D, as shown in the equation below:

$$D = \frac{[\mathrm{Ni\ (II)}]_{CPL}}{[\mathrm{Ni\ (II)}]_{aq}} \tag{1}$$

3. Results and discussion

3.1. UV-visible spectroscopy

10 mL aqueous solutions containing the reagents HQDBS or IDQ with a concentration of 1×10^{-3}M were mixed with Ni (II) ion with a concentration of 100 µg/mL, adjusting the pH of the solution to 9, then adding 0.5 mL Triton X100. The solutions were heated at 80°C for 15 min. Then, the cloud point layer was dissolved in 5 mL of ethanol. The spectra of the colored complex were taken against the reagent solution as a blank solution. **Figures 1a-b** show the UV-Vis absorption spectra of the Ni (II) chelation complexes with HQDBS and IDQ, which have a maximum wavelength of 480 nm with HQDBS and 484 nm with IDQ. The spectra in **Figure 1a** and **b** displayed a peak at 397 nm and 390 nm for the reagents due to the (π-π*) electron transfer. Upon the complexation of the reagents HQDBS and IDQ with Ni (II) ion, a new peak appeared at 480 nm and 484 nm related to (n-π*) electron transfer. This change in electronic transition confirms the formation of the Ni (II) complexes with the reagents HQDBS and IDQ [37].

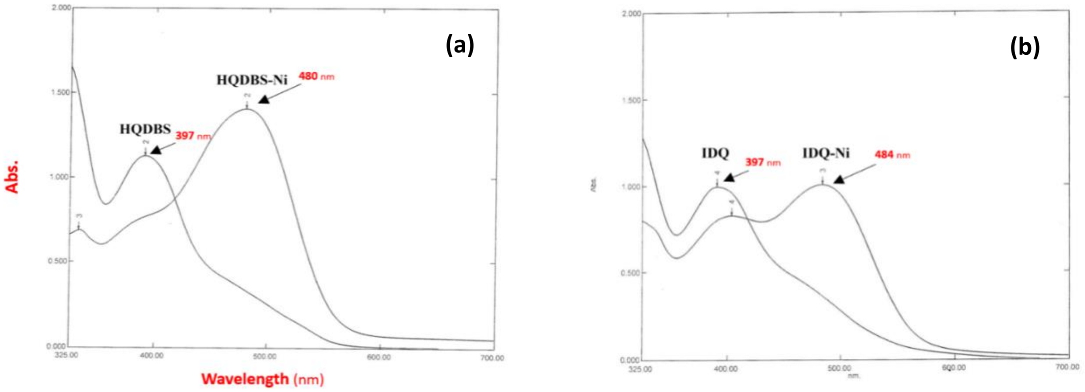

Figure 1. UV-visible spectra of (a) HQDBS and Ni (II) HQDBS complex and (b) IDQ and Ni (II) IDQ complex.

3.2. Fourier transform infrared (FT-IR) spectroscopy for the reagents

The FT-IR spectrum of the reagent (HQDBS) in **Figure 2** signifies the following characteristic absorption bands: ν 3334, 3238 cm^{-1} (s) of primary amine sulfonamide (NH_2) overlap with phenol group (OH); ν 3080 cm^{-1} (s) of (Ar. C-H); ν 1759 cm^{-1} (s) of (C=N, cyclic); ν 1504 cm^{-1} (s) of (Ar. C=C band); ν 1405 cm^{-1} (s) of azo group (N=N); ν 1292, 1153 cm^{-1} (s) of (S=O)[37-39].

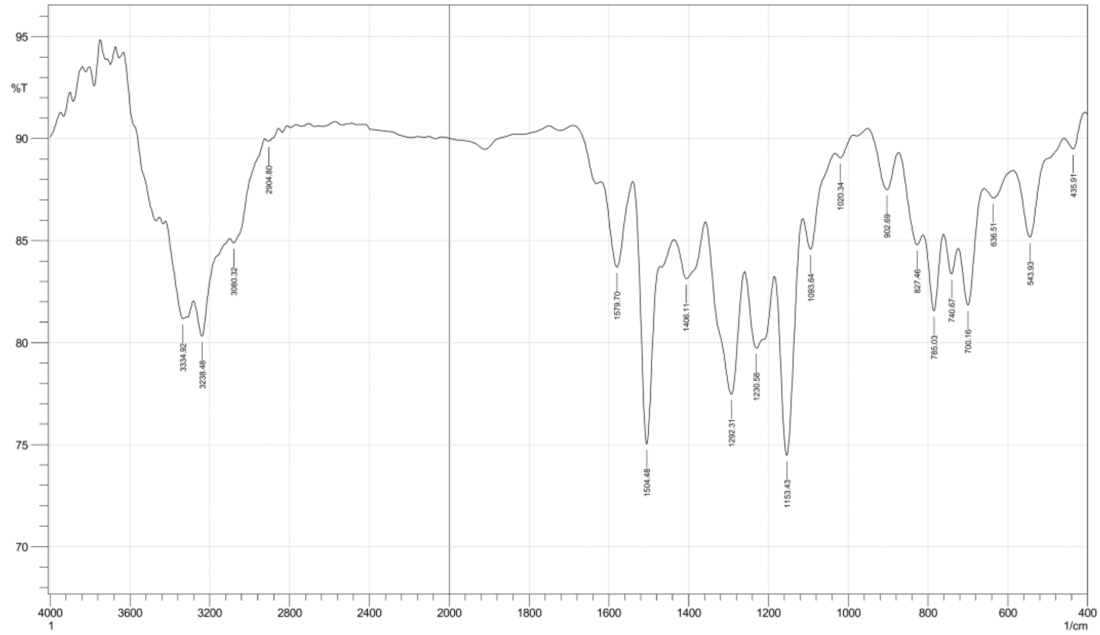

Figure 2. FT-IR spectrum of the reagent, HQDBS.

The FT-IR spectrum of the reagent, IDQ, **Figure 3**, signifies the following characteristic absorption bands: ν 3188 cm⁻¹ (s) of secondary amine (NH) overlap with phenol group (OH); ν 3053 cm⁻¹ (s) of (Ar. C-H); 1579 cm⁻¹ (s) of (C=N, cyclic); ν 1502, 1471 cm⁻¹ (s) of C=C); ν 1409 cm⁻¹ (s) of azo group (N=N) [40-42].

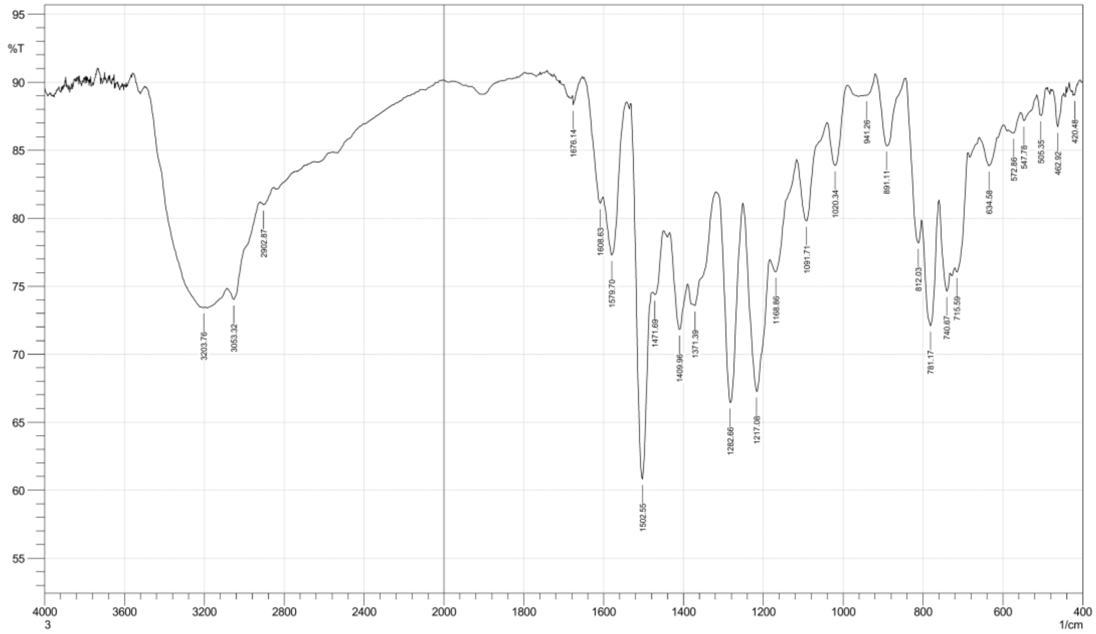

Figure 3. FT-IR spectrum of reagent, IDQ.

3.3. ^{1}H-NMR spectroscopy and FE-SEM analysis

The ^{1}H-NMR spectrum of reagent, HQDBS (**Figure 4**) signifies δ 7.3 ppm (s, 2H, NH_2) for amine; δ 7.5-8.5 ppm multiplet signals result from overlapping of nonequivalent aromatic protons; δ 8.3 ppm (s, 1H, HC=N cyclic); δ 9.9 ppm (s, 1H, OH).

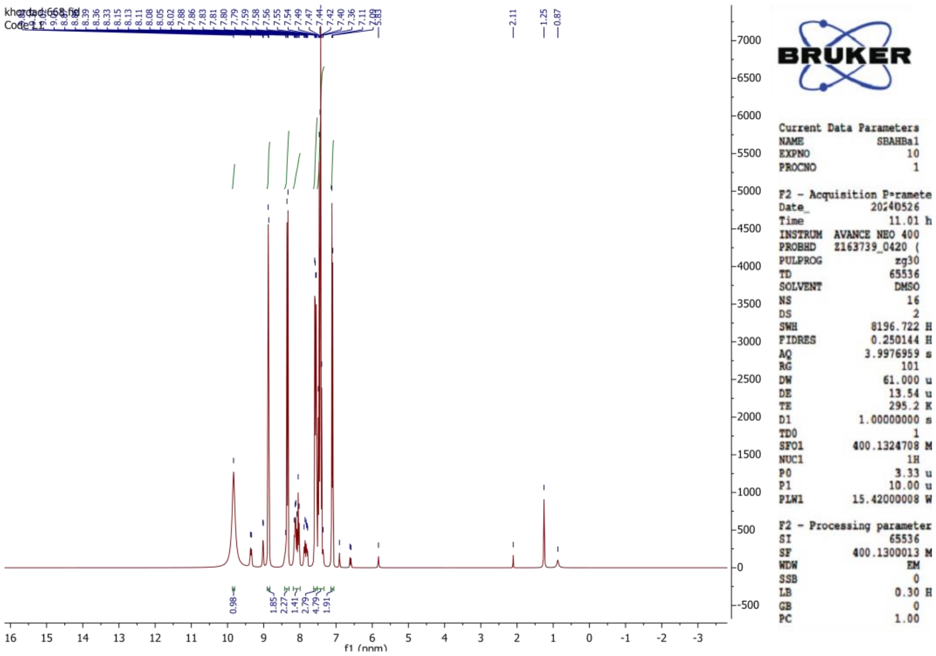

```
Current Data Parameters
NAME             SBAHBa1
EXPNO                 10
PROCNO                 1

F2 - Acquisition Paramete
Date_           20240526
Time               11.01 h
INSTRUM   AVANCE NEO 400
PROBHD    Z163739_0420 (
PULPROG             zg30
TD                 65536
SOLVENT             DMSO
NS                    16
DS                     2
SWH             8196.722 H
FIDRES          0.250144 H
AQ             3.9976959 s
RG                   101
DW                61.000 u
DE                 13.54 u
TE                 295.2 K
D1            1.00000000 s
TD0                    1
SFO1         400.1324708 M
NUC1                  1H
P0                  3.33 u
P1                 10.00 u
PLW1         15.42000008 W

F2 - Processing parameter
SI                 65536
SF           400.1300013 M
WDW                   EM
SSB                    0
LB                  0.30 H
GB                     0
PC                  1.00
```

Figure 4a. ^{1}H-NMR spectrum of reagent HQDBS.

However, the ^{1}H-NMR spectrum of the reagent, IDQ in **Figure 4b** signifies δ 6.5-7 ppm (2H, HC=CH, cyclic); δ 7.3-9 ppm multiplet signals result from the overlapping of nonequivalent aromatic protons; δ 9.8 ppm (s, 1H, OH); δ 11 ppm (s, 1H, NH cyclic)[40].

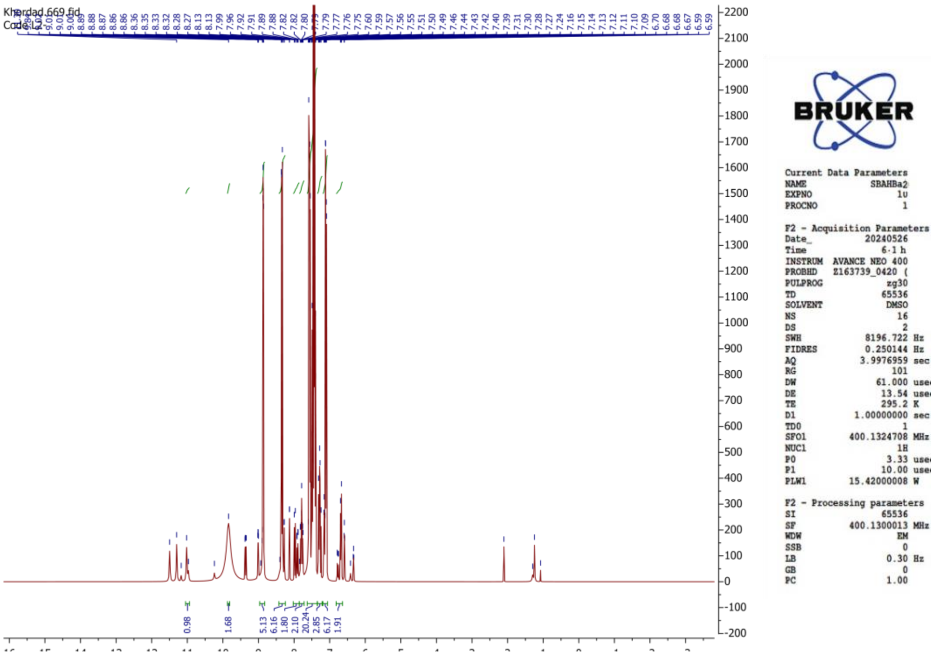

```
Current Data Parameters
NAME              SBAHBa2
EXPNO                  10
PROCNO                  1

F2 - Acquisition Parameters
Date_            20240526
Time                6.1 h
INSTRUM   AVANCE NEO 400
PROBHD    Z163739_0420 (
PULPROG              zg30
TD                  65536
SOLVENT              DMSO
NS                     16
DS                      2
SWH              8196.722 Hz
FIDRES           0.250144 Hz
AQ              3.9976959 sec
RG                    101
DW                 61.000 use
DE                  13.54 use
TE                  295.2 K
D1             1.00000000 sec
TD0                     1
SFO1          400.1324708 MHz
NUC1                   1H
P0                   3.33 use
P1                  10.00 use
PLW1          15.42000008 W

F2 - Processing parameters
SI                  65536
SF            400.1300013 MHz
WDW                    EM
SSB                     0
LB                   0.30 Hz
GB                      0
PC                   1.00
```

Figure 4b. ^{1}H-NMR spectrum of reagent IDQ.

The surface morphology of Ni (II) extracted complexes with HQDBS and IDQ, and the surfactant TritonX-100 was investigated. SEM imaging of Triton X-100 in Cloud Point Extraction (CPE) usually focuses on capturing the morphology of surfactant-rich phase, micelles, or any extracted nanoparticles. However, since Triton X-100 is a nonionic surfactant and forms a liquid phase, direct imaging of its pure form can be challenging. The **Figure 5a-c** show embedded Ni (II) ions complexes with HQDBS and IDQ in the surfactant matrix[43,44].

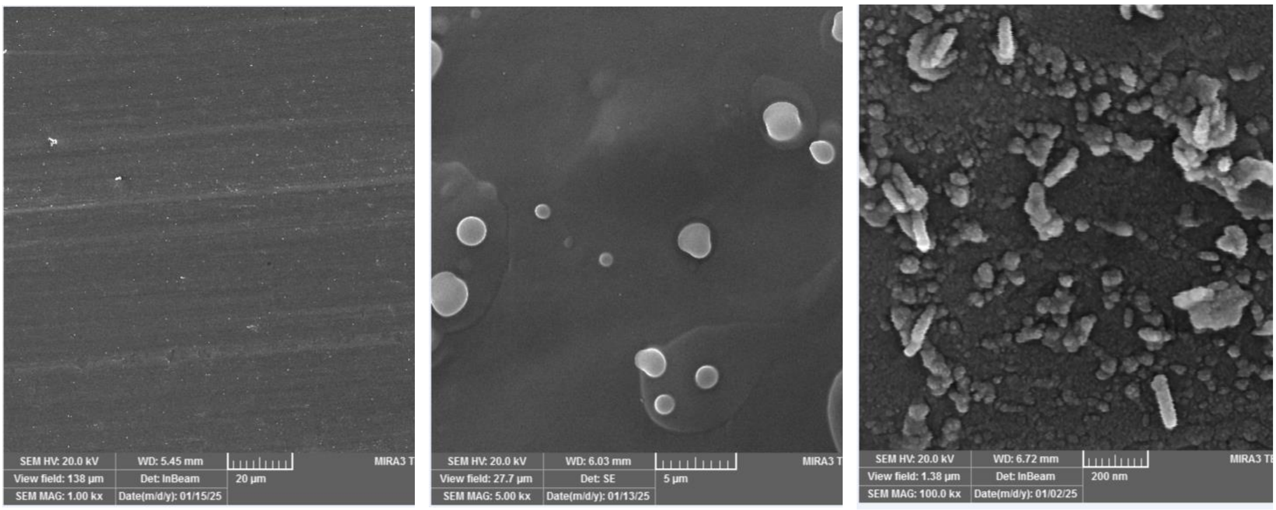

(a)

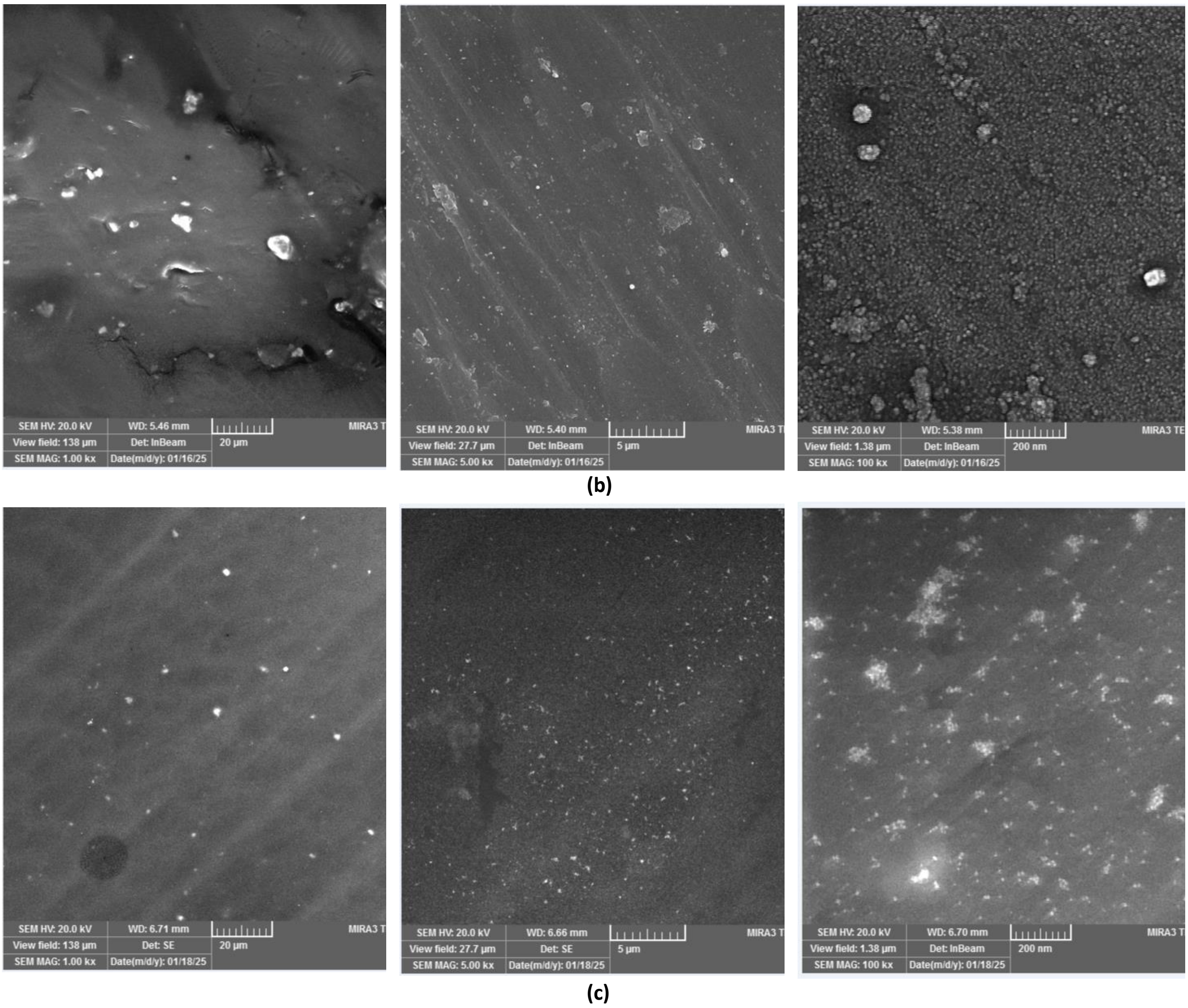

Figure 5. FE-SEM of (a) TritonX-100, (b) Ni (II)-HQDBS and (c) Ni (II)-IDQ.

3.4. Optimal conditions

3.4.1. Effect of pH and temperature

100µg of Ni (II) was extracted in 10 mL of aqueous solution at different pH values in the presence of 1×10^{-4} M of HQDBS or IDQ, each one alone. The solutions were heated for 15 minutes to a suitable temperature, as indicated in the general procedure. The experimental outcomes (**Figure 6a-b**) revealed that the optimal pH values for higher extraction efficiency of Ni (II) with HQDBS and IDQ were 8 and 9, respectively. At these pH values, reaching the maximum rate of thermodynamic equilibrium forward direction is for forming chelation complexes of Ni (II) with the best distribution ratio D into the cloud point layer because, at these pH values, gate favorable coordinately binding between organic reagents and Ni (II) with higher stability at any pH is less than optimal value. It does not arrive at the finest equilibrium and declines extraction efficiency at a pH value higher than the optimum. Extraction efficiency decreases by forming a stable compound between metal and hydroxyl ions in aqueous solution[45,46].

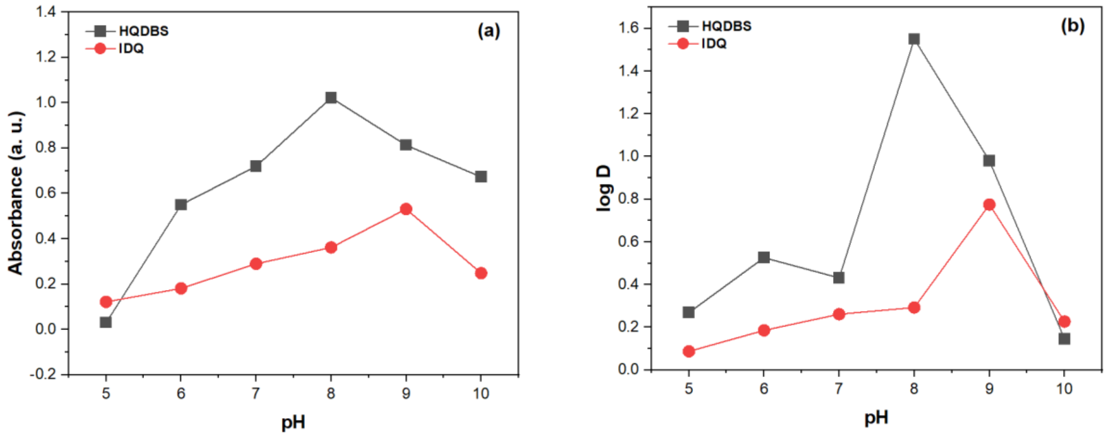

Figure 6. Effect of pH on (a) absorbance and (b) extraction efficiency and D-values.

One of the main factors influencing how systems with nonionic surfactants behave is the temperature of the CPE process. Water droplets cause the separation phenomenon formed when the temperature rises, making the surfactant more hydrophobic. On the other hand, the amount and composition of the surfactant in use determine the separation temperature. The temperature impact was examined for 15 minutes in 70 °C to 95 °C range to find optimal temperature for process. **Figure 7a-b** and **Table 1** show that the ideal temperature for a satisfactory Ni (II) ion extraction with HQDBS is 80°C. In contrast, the best temperature for a Ni (II) ion extraction with IDQ is 90°C, which will supply the energy required together the surfactant micelles, eliminate water molecules, and create a CPL with the perfect properties for the precise extraction of Ni (II) chelation complexes[47]. The extraction constant K_{ex} (**Figure 7c**) at every temperature was calculated by applying the relation below:

$$K_{ex} = \frac{D}{[Ni\ (JJ)][R]} \tag{2}$$

here, R = HQDBS and IDQ.

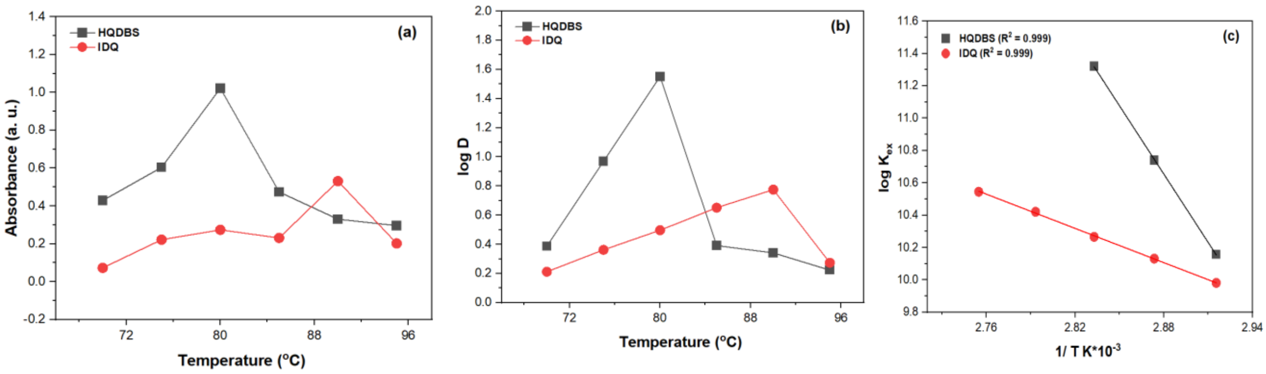

Figure 7. Effect of pH on (a) absorbance, (b) extraction efficiency and D-values and (c) relation between extraction constant and temperature.

Table 1. Thermodynamic parameters of Ni (II) complexes.

Complex	**(Δlog K_{ex} / Δ1/T) = Slope = (-ΔH_{ex} / 2.303R)**		
	ΔH_{ex} (kJ.mol^{-1})	**ΔG_{ex} = -R T Ln K_{ex} (kJ.mol^{-1})**	**ΔS_{ex} (J.mol^{-1}K^{-1})**
HQDBS	269.71	-76.501	980.76
IDQ	67.531	-73.278	387.9

3.4.2. Effect of heating time and surfactant volume

The duration of heating in cloud point extraction should be adjusted to optimize the extraction process for maximum analyte recovery and selectivity. If the heating time is too short, incomplete phase separation may result in lower extraction efficiency. On the other hand, excessively long heating times can lead to degradation of the analyte or surfactant, which can compromise the accuracy of the results. The heating time varied from 10 to 25 min. **Figure 8a-b** revealed that heating the solution for 15 min was the best time for achieving excellent extraction efficiency with both reagents. Heating solution for longer than the optimal time decreased the extraction efficiency due to the effect of diffusion of micelles in aqueous solution[47].

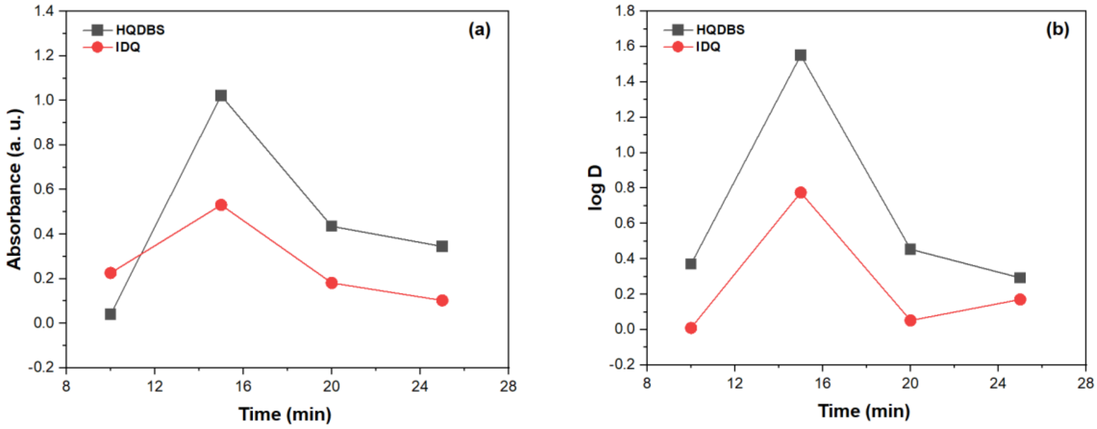

Figure 8. Effect of time on (a) absorbance and (b) extraction efficiency and D-values.

Optimizing surfactant volume is crucial for maximizing CPE performance and achieving high analyte recovery. In the experimental setup, evaluated volumes of TritonX-100 ranged from 0.1 to 1.0 mL. The optimal volumes for higher extraction efficiency were 0.8 mL and 0.5 mL of TritonX-100 for Ni(ll) with HQDBS and IDQ, respectively (**Figure 9a-b**). Optimum volumes are suitable for higher extraction efficiency of Ni (II) because this volume achieved a CMC state.

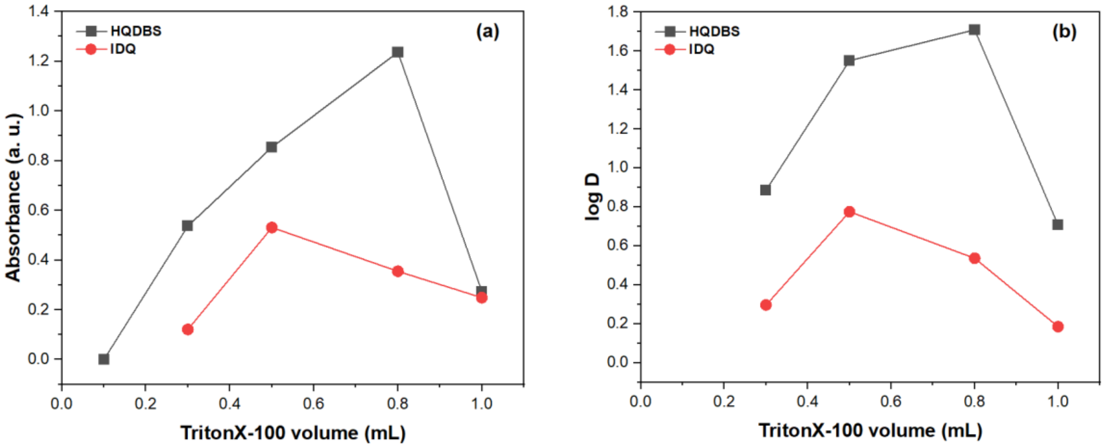

Figure 9. Effect of TritonX-100 volume (mL) on (a) absorbance and (b) extraction efficiency and D-values.

3.5. Structure of extracted complexes

The mole ratio approach, applied under optimal conditions and following standard procedures, indicates the likely structure of chelate complexes extracted into CPL. The findings demonstrated in **Figure 10a-b** illustrate the probable structure of isolated Ni (II) complexes with two organic reagents.

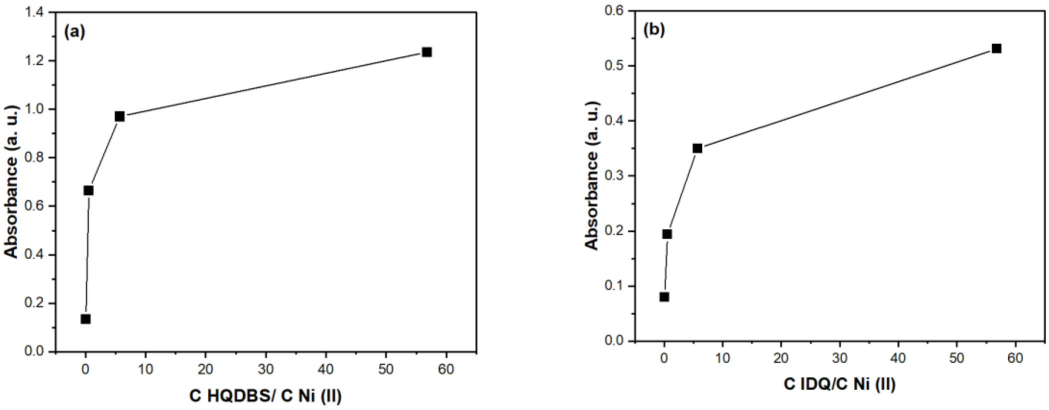

Figure 10. Mole ratio of (a) Ni-HQDBS complex and (b) Ni-IDQ complex.

The mole ratio values were 0.8 and 0.85 for Ni-HQBDS and Ni-IDQ, respectively, demonstrating that the more probable structure of chelate-extracted complexes into CPL was 1:1, as illustrated in **Figure 11**.

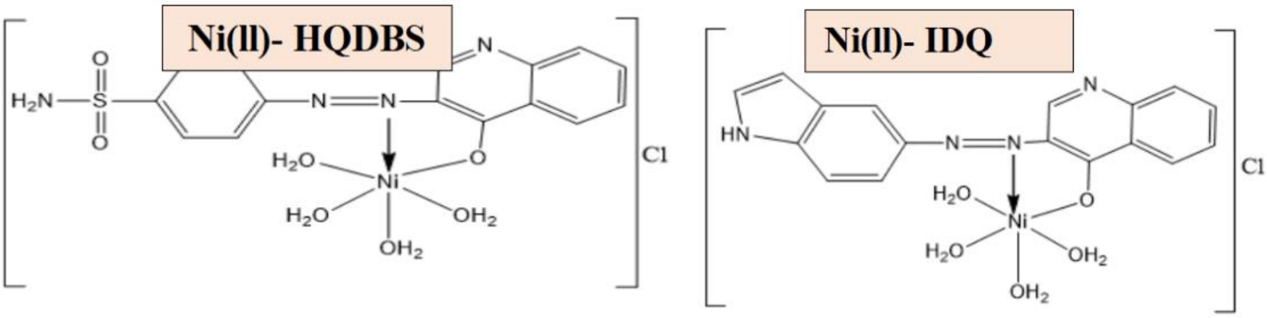

Figure 11. Structure of extracted complexes.

3.6. Influence of ionic strength

Ni (II) was extracted at optimum conditions according to procedure and in some electrolyte salts in aqueous solution at 0.01 M. The experimental results are listed in **Table 2**. The results depict an enhancement in the extraction efficiency of electrolytes in aqueous solution. Because of the effect of destroying the hydration shell of Ni (II) ion, the chances of binding with HQDBS and IDQ are increased to form chelation complexes, and this increase in extraction efficiency varies with different electrolytes according to their performance in aqueous solution.

Table 2. Effect of electrolyte on extraction efficiency of Ni^{+2} with HQDBS and IDQ.

Electrolyte	Ionic Strength	Absorbance at λ_{max} = 480 nm (HQDBS)	D (HQDBS)	Absorbance at λ_{max} = 484nm (IDQ)	D (IDQ)
Without	-	1.236	51.128	0.531	5.96
KCl	0.01	1.541	57.333	1.273	9.338
NaCl	0.01	1.823	46.115	1.378	10.836
LiCl	0.01	1.648	65.216	1.381	12.462
NH_4Cl	0.01	0.743	12.462	0.228	3.209
Ca $(NO_3)_2.4H_2O$	0.02	0.911	3.104	0.271	3.605

3.7. Interferences

Extracted Ni (II) was used following to the procedure in the presence of foreign metal ions at 0.01 M. Results (**Table 3**) show different interferences with foreign ions in an aqueous solution because these ions could form chelation complexes with organic reagents HQDBS and IDQ[48].

Table 3. Influence of interferences on extraction efficiency of HQDBS and IDQ.

Foreign Ions	Abs. at λmax=480nm (Ni(II)+HQDBS)	D (Ni(II)+HQDBS)	Abs. at λmax=484nm (Ni(II)+IDQ)	D (Ni(II)+IDQ)
Co (II)	0.543	0.334	0.407	1.352
Cd (II)	0.576	1.164	0.337	0.594
Pb (II)	0.726	1.778	0.3	1.363
Cr (III)	0.41	1.127	0.402	0.711
Hg (II)	0.715	2.258	0.307	0.711
Cu (II)	0.165	1.482	0.458	0.934

4. Spectrophotometric determination of Nickel (II) ions in different samples

4.1. Calibration curve of Ni (II)

The calibration curve for Ni (II) was obtained by applying the general procedure at varying Ni (II) concentrations under optimum conditions, as shown in **Figure 12**. The calibration curve parameters are detailed in **Table 4**.

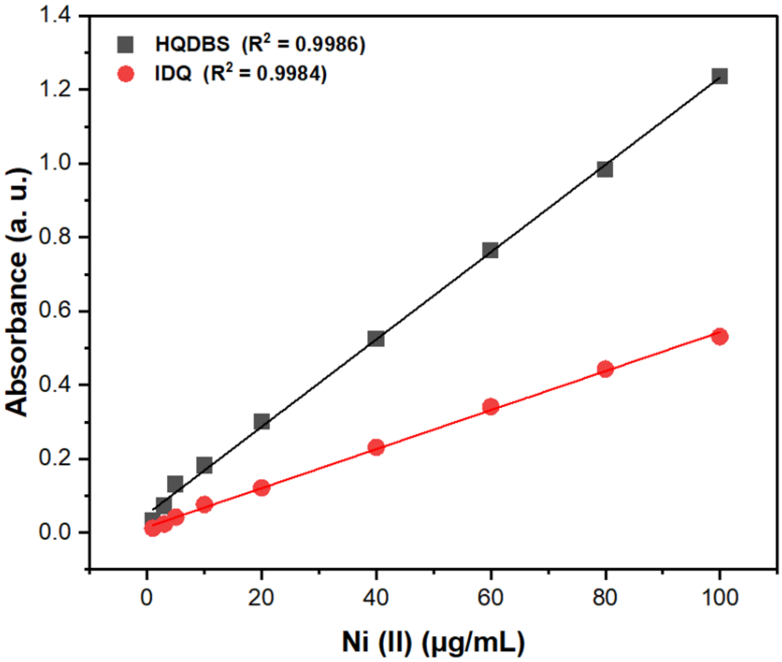

Figure 12. Calibration curves of Ni (II) using HQDBS and IDQ.

Table 4. Parameters for determination of Ni (II) using HQDBS and IDQ.

Parameter	HQDBS	IDQ
λ_{max} (nm)	480	484
Beer's law obeys (ppm)	1-100	1-100
Molar absorptivity (L/mol/cm)	6.941 x 10^3	3.100 x 10^3
Limit of Detection (μg/mL^{-1})	0.1749	0.1933
Limit of Quantity (μg/mL^{-1})	0.5303	0.5858

4.2. Applications

The procedure was finally utilized to determine Ni (II) levels in six food samples obtained from a local market. The sample was treated with a wet digestion method[49]. **Table 5** shows the results obtained using proposed CPE and flame atomic absorption spectroscopy (FAAS). The strong agreement between the procedure and direct analysis by FAAS indicates that this technique may be suitable for determining the Ni (II) levels in various samples. Results of statistical analysis for both CPE and FAAS methods revealed that all p-values [$P(F_{cal.} < F_{crt.})$ two-tailed] determined by the 5 % critical value of 5.05 (F-critical) surpassed the F-calculated values. These results revealed that null hypothesis (H_o) can be acceptable highlighting no substantial difference between CPE and FAAS techniques.

Table 5. Determination of Ni (II) via CPE and comparison with FAAS.

	Sample Name	**Ni (II) amount (CPE)**	**Ni (II) amount (FAAS)**	**Parameter**	**Value**
Ni (II) Determination	Apricot	0.811	0.746	Mean (CPE)	5.95
	Onion	20.4	19.23	Mean (FAAS)	6.135
	Lentils	2.87	2.91	Variance (CPE)	63.228
	Cashew nuts	0.994	0.956	Variance (FAAS)	61.9788
	Cocoa powder	10.11	12.48	Observations (n)	6
	Banana	0.512	0.488	Degrees of Freedom (df)	5
				F-statistic	1.02
				P(F<=f) one-tail	0.492
				F Critical one-tail	5.05

4. Conclusion

The study involved the utilization of a new method that makes use of 4-((4-hydroxyquinolin-3-yl)diazenyl)benzenesulfonamide (HQDBS) and 3-((1H-indol-5-yl)diazenyl)quinolin-4-ol (IDQ) for the synthesis of stable chelate complexes. For the highly efficient extraction of Ni (II), cloud point extraction (CPE) method was combined with liquid ion exchange by making the use of a surfactant i.e., Triton X-100. Different techniques including UV-Vis, FTIR, and 1H-NMR were used for the analysis. Results of the effect of different electrolytes, pH, time, ionic strength revealed that the studied method is still reliable and can be effective under the changing experimental conditions. At the end, the results of the study were best matched with flame atomic absorption spectroscopy (FAAS) findings that further validates the reliability of the studied process.

Author contributions

Authors contributed equally to the manuscript.

Acknowledgments

Authors are grateful to both Dr. Sahar Al-Assam as well as Dr. Rana Al-Mousawi due to their help and guidance.

Conflict of interest

The authors declare no conflict of interest

References

1. Awual, M.E., et al., Ligand imprinted composite adsorbent for effective Ni (II) ion monitoring and removal from contaminated water. Journal of Industrial and Engineering Chemistry, 2024. 131: p. 585-592.
2. Shah, A., et al., Removal of cadmium and zinc from water using Sewage sludge-derived biochar. Sustainable Chemistry for the Environment, 2024.
3. Shah, A., et al., Adsorptive removal of arsenic from drinking water using KOH-modified sewage sludge-derived biochar. Cleaner Water, 2024: p. 100022.

4. Awual, M.R., A facile composite material for enhanced cadmium (II) ion capturing from wastewater. Journal of Environmental Chemical Engineering, 2019. 7(5): p. 103378.
5. Naveed, M., et al., Applications of heavy metal-based nanoparticles in cosmetics: a comprehensive review. Cutaneous and Ocular Toxicology: p. 1-18.
6. Mahdi, Z., A. El Hanandeh, and Q.J. Yu, Preparation, characterization and application of surface modified biochar from date seed for improved lead, copper, and nickel removal from aqueous solutions. Journal of Environmental Chemical Engineering, 2019. 7(5): p. 103379.
7. Taher, A., et al., Applications of Nano Composites for Heavy Metal Removal from Water by Adsorption: Mini Review. Journal of Nanostructures, 2024. 14(4): p. 1239-1251.
8. Thabede, P.M., et al., Adsorption studies of toxic cadmium (II) and chromium (VI) ions from aqueous solution by activated black cumin (Nigella sativa) seeds. Journal of Environmental Chemical Engineering, 2020. 8(4): p. 104045.
9. Yasmeen, H., et al., Visible light-excited surface plasmon resonance charge transfer significantly improves the photocatalytic activities of ZnO semiconductor for pollutants degradation. Journal of the Chinese Chemical Society, 2020. 67(9): p. 1611-1617.
10. Rehan, A.I., et al., Improving toxic dye removal and remediation using novel nanocomposite fibrous adsorbent. Colloids and Surfaces A: Physicochemical and Engineering Aspects, 2023. 673: p. 131859.
11. Shah, A., et al., Sequential novel use of Moringa oleifera Lam., biochar, and sand to remove turbidity, E. coli, and heavy metals from drinking water. Cleaner Water, 2024: p. 100050.
12. Alshamusi, Q.K.M., et al., Efficiency of Chitosan-Grafted Poly (Carboxymethyl Cellulose-Co-Acrylamide) Nano Hydrogel for Cadmium (II) Removal: Batch Adsorption Study. Journal of Nanostructures, 2024. 14(4): p. 1122-1133.
13. Xue, Y., et al., Nickel removal by the two-step synthesis of ceramsite from sediments and water hyacinth. Journal of Environmental Chemical Engineering, 2023. 11(4): p. 110325.
14. Hamid, M.M., R.F. Shahad, and M.T.A. Almekh, Assessment of Groundwater Quality and Suitability for Irrigation Purpose in Northern Babil Governorate. Journal of Environmental and Earth Sciences, 2025. 7(4): p. 368-377.
15. Shahad, R.F. and M.M. Hamid, Impact of Bentonite and Humic Acid on the Growth and Flowering of Catharanthus roseus L. in Sandy Soil. Journal of Environmental and Earth Sciences, 2025. 7(1): p. 157-166.
16. Jamel, H.O., et al., Adsorption of Rhodamine B dye from solution using 3-((1-(4-((1H-benzo[d]imidazol-2-yl)amino)phenyl)ethylidene)amino)phenol (BIAPEHB)/ P(AA-co-AM) composite. Desalination and Water Treatment, 2025: p. 101019.
17. Majeed, H.J., et al., Synthesis and application of novel sodium carboxy methyl cellulose-g-poly acrylic acid carbon dots hydrogel nanocomposite (NaCMC-g-PAAc/CDs) for adsorptive removal of malachite green dye. Desalination and Water Treatment, 2024. 320: p. 100822.
18. Mohamed, G., et al., Synthesis and characterization of porous magnetite nanosphere iron oxide as a novel adsorbent of anionic dyes removal from aqueous solution. Biointerface Res. Appl. Chem, 2021. 11: p. 13377-13401.
19. El-Bindary, M., et al., Spectrophotometric and fluorometric methods for effective monitoring of rust state in boiler systems and Fe2+ ion in pharmaceutical samples. Journal of Molecular Liquids, 2023. 382: p. 121946.
20. Awual, M.R., et al., Green and robust adsorption and recovery of Europium (III) with a mechanism using hybrid donor conjugate materials. Separation and Purification Technology, 2023. 319: p. 124088.
21. Waliullah, R., et al., Optimization of toxic dye removal from contaminated water using chitosan-grafted novel nanocomposite adsorbent. Journal of Molecular Liquids, 2023. 388: p. 122763.
22. Javed, T., et al., Batch adsorption study of Congo Red dye using unmodified Azadirachta indica leaves: isotherms and kinetics. Water Practice & Technology, 2024: p. wpt2024020.
23. Bezerra, M.A., et al., Multivariate optimization of a procedure for Cr and Co ultratrace determination in vegetal samples using GF AAS after cloud-point extraction. International Journal of Environmental and Analytical Chemistry, 2008. 88(2): p. 131-140.
24. Lemos, V.A., R.S. da França, and B.O. Moreira, Cloud point extraction for Co and Ni determination in water samples by flame atomic absorption spectrometry. Separation and Purification Technology, 2007. 54(3): p. 349-354.
25. Aranda, P.R., et al., Cloud point extraction of mercury with PONPE 7.5 prior to its determination in biological samples by ETAAS. Talanta, 2008. 75(1): p. 307-311.
26. Yamini, Y., et al., On-line metals preconcentration and simultaneous determination using cloud point extraction and inductively coupled plasma optical emission spectrometry in water samples. analytica chimica acta, 2008. 612(2): p. 144-151.
27. Hussain, S.A., et al., Separation, Pre-concentration, and Determination of Al (III) by Cloud Point Extraction as a Compact Method with Liquid Ion Exchange. 2023.
28. Gilani, A.G., et al., Solvatochromism and dichroism of fluorinated azoquinolin-8-ol dyes in liquid and liquid crystalline solutions. Journal of Molecular Liquids, 2008. 139(1-3): p. 72-79.

29. Gilani, A.G., et al., Tautomerism, solvatochromism, preferential solvation, and density functional study of some heteroarylazo dyes. Journal of Molecular Liquids, 2019. 273: p. 392-407.
30. Karcı, F., et al., Synthesis of 4-amino-1H-benzo [4, 5] imidazo [1, 2-a] pyrimidin-2-one and its disperse azo dyes. Part 1: Phenylazo derivatives. Dyes and Pigments, 2006. 71(2): p. 90-96.
31. Al-Adilee, K. and H.A. Kyhoiesh, Preparation and identification of some metal complexes with new heterocyclic azo dye ligand 2-[2−-(1-Hydroxy-4-Chloro phenyl) azo]-imidazole and their spectral and thermal studies. Journal of Molecular Structure, 2017. 1137: p. 160-178.
32. Mahmoud, A., et al., Telaprevir is a potential drug for repurposing against SARS-CoV-2: computational and in vitro studies. Heliyon, 2021. 7(9).
33. Mezgebe, K. and E. Mulugeta, Synthesis and pharmacological activities of azo dye derivatives incorporating heterocyclic scaffolds: a review. RSC advances, 2022. 12(40): p. 25932-25946.
34. Kyhoiesh, H.A.K. and K.J. Al-Adilee, Pt (IV) and Au (III) complexes with tridentate-benzothiazole based ligand: synthesis, characterization, biological applications (antibacterial, antifungal, antioxidant, anticancer and molecular docking) and DFT calculation. Inorganica Chimica Acta, 2023. 555: p. 121598.
35. Alabidi, H.M., A.M. Farhan, and M.M. Al-Rufaie, Spectrophotometric determination of Zn (II) in pharmaceutical formulation using a new Azo reagent as derivative of 2-naphthol. Current Applied Science and Technology, 2021: p. 176-187.
36. Ali, S. and I.R. Ali, Cloud point extraction and determination of Nickel (II) ions complex in real samples using New azo reagent. Adv. Sci, 2020. 1(2): p. 7-18.
37. Francisco, K.R., et al., Structure property relationships of N-acylsulfonamides and related bioisosteres. European journal of medicinal chemistry, 2021. 218: p. 113399.
38. Shahad, R.F., A.M. Abdullah, and S.K. Essa, Studying the Effect of Agriculturally Exploited Soils on the Transformation of Mica Minerals using Infrared Spectroscopy (IR). Malaysian Journal of Chemistry, 2021. 23(4): p. 144-153.
39. Mahdi, M.A., et al., Tailoring the innovative Lu2CrMnO6 double perovskite nanostructure as an efficient electrode materials for electrochemical hydrogen storage application. Journal of Energy Storage, 2024. 88.
40. Palchykov, V.A. and A.A. Gaponov, 1, 3-Amino alcohols and their phenol analogs in heterocyclization reactions. Advances in Heterocyclic Chemistry, 2020. 131: p. 285-350.
41. Kianipour, S., et al., The synthesis of the P/N-type NdCoO3/g-C3N4 nano-heterojunction as a high-performance photocatalyst for the enhanced photocatalytic degradation of pollutants under visible-light irradiation. Arabian Journal of Chemistry, 2022. 15(6).
42. Razavi, F.S., et al., Fabrication and design of four-component Bi2S3/CuFe2O4/CuO/Cu2O nanocomposite as new active materials for high performance electrochemical hydrogen storage application. Journal of Energy Storage, 2024. 94.
43. Samaddar, P. and K. Sen, Cloud point extraction: A sustainable method of elemental preconcentration and speciation. Journal of Industrial and Engineering Chemistry, 2014. 20(4): p. 1209-1219.
44. Yoo, N.-K., Y.-R. Jeon, and S.-J. Choi, Determination of two differently manufactured silicon dioxide nanoparticles by cloud point extraction approach in intestinal cells, intestinal barriers and tissues. International journal of molecular sciences, 2021. 22(13): p. 7035.
45. Marczenko, Z. and M. Balcerzak, Separation, preconcentration and spectrophotometry in inorganic analysis. Vol. 10. 2000: Elsevier.
46. Jawad, S.K., et al., Solvent extraction of copper (II) from aqueous solutions by new organic reagent 2-[(3-Hydroxy phenyl) azo]-4, 5-diphenyl imidazole. Al-Qadisiyah Journal of Pure Science, 2013. 18(1).
47. Mortada, W.I., Recent developments and applications of cloud point extraction: A critical review. Microchemical Journal, 2020. 157: p. 105055.
48. Jawad, S.K. and A.S. Abed, Efficient Method Cloud Point Extraction for Separation Preconcentration and Trace amount Determination of Bismuth (III) from Different Samples by New Laboratory Prepared Azo Derivative. J. of Natural Sciences Research, 2015. 5(7): p. 39-51.
49. Yang, K., et al., Determination of trace elements in animal feed by wet digestion and atomic absorption spectrometry. 2023.